Identification of *SULF2* as a Novel Transcriptional Target of p53 by Use of Integrated Genomic Analyses

B. Nelson Chau, Robert L. Diaz, Matthew A. Saunders, Chun Cheng, Aaron N. Chang, Paul Warrener, Jeffrey Bradshaw, Peter S. Linsley, and Michele A. Cleary

Rosetta Inpharmatics LLC, a wholly owned subsidiary of Merck & Co., Inc., Seattle, Washington

Abstract

Microarray analysis has been useful for identifying the targets of many transcription factors. However, gene expression changes in response to transcription factor perturbation reveal both direct transcriptional targets and secondary gene regulation. By integrating RNA interference, gene expression profiling, and chromatin immunoprecipitation technologies, we identified a set of 32 direct transcriptional targets of the tumor suppressor p53. Of these 32 genes, 11 are not currently associated with the core p53 pathway. From among these novel pathway members, we focused on understanding the connection between p53 and *SULF2*, which encodes an extracellular heparan sulfate 6-*O*-endosulfatase that modulates the binding of growth factors to their cognate receptors and that has been shown to function as a tumor suppressor. Genetic and pharmacologic perturbation of p53 directly influences *SULF2* expression, and similar to silencing of *TP53*, RNA interference–mediated suppression of *SULF2* results in an impaired senescence response of cells to genotoxic stress. Thus, our integrated genomic approach has led to the identification of a novel mediator of p53 network biology. [Cancer Res 2009;69(4):1368–74]

Introduction

Dysregulation of the p53 tumor suppressor pathway interferes with tissue homeostasis, primes cells for tumorigenesis, and is associated with chemotherapy and radiotherapy resistance (1–3). p53 regulates expression of a large network of genes through transcriptional activation. Although the list of p53 downstream effectors that mediate its tumor suppressor function by inducing cell cycle arrest, apoptosis, and senescence is sizable (4–6), therapeutic strategies for cancer around these targets have been limited. Microarray-based gene expression analyses are frequently used to identify potential downstream targets of transcription factors. For p53, gene expression profiling experiments with different modes of activating p53 function have identified overlapping, yet distinct, sets of potential downstream p53 targets (6, 7). However, gene expression profiling reports both direct transcriptional and indirect secondary targets. Overall, systematic validation of direct targets in these previous studies has not been rigorously pursued.

To identify a list of direct transcriptional targets of p53 with high confidence, we interrogated the pathway by use of several genomic technologies and RNA interference (RNAi). RNAi is effective for the engineering of paired cell lines of identical genetic background with and without a defined gene deficiency. To identify changes in the transcriptome that result specifically from perturbation of the p53 pathway, we generated a panel of matched-pair and inducible p53 knockdown cell lines of multiple cancer origins and compared their gene expression profiles. From these steps, we established a set of consensus genes that universally responded to the perturbation of p53. To distinguish direct from indirect targets, we performed chromatin immunoprecipitation (ChIP) surveying both the whole genome and focused loci. Additionally, we confirmed the presence of p53 recognition sites in gene promoters by use of an algorithm that identifies and ranks potential p53 interacting sequences (7). Combining the results from these approaches, we identified a high confidence list of genes that are directly regulated by p53.

Among this set of p53 direct targets, there are known, as well as novel, p53 transcriptional targets. We present results of our follow-up on one such novel pathway member, SULF2. SULF2 and the related protein SULF1 are extracellular heparan sulfate 6-*O*-endosulfatases that share similar substrate specificity and perform redundant physiologic functions (8). SULF1 and SULF2 remove the sulfate group from the polysaccharide side chain of heparan sulfate proteoglycans and modulate the activity of several signaling proteins including fibroblast growth factors, bone morphogenic proteins, and WNTs (8–12). Relevant to having a role in the p53 pathway, loss of SULF1 and SULF2 has been reported in several types of cancers, and emerging evidence suggests that sulfatases function as tumor suppressors (13–15).

By integrating gene expression profiling, ChIP, and transcription factor binding site prediction, we have effectively identified a "highly interrogated" list of direct downstream targets of an important cancer relevant transcription factor, p53. Furthermore, we have validated *SULF2* as a direct transcriptional target of p53 and have provided evidence that SULF2 protein mediates some aspect of p53 function—DNA damage–induced senescence.

Materials and Methods

Plasmids and sequences. pENTR, pLenti6-Block-IT, and pLenti4-Block-IT plasmids were obtained from Invitrogen. Tet repressor (tT-R) has been previously described (16). An shRNA targeting the *TP53* transcript (p53-1026sh; GACTCCAGTGGTAATCTACTTCAAGAGAGTAGATTACCACTG-GAGTCT) was subcloned 3′ to an H1 promoter in the pENTR plasmid. To generate inducible shRNA expression plasmids, a TetR binding site (x7) was subcloned 5′ to the H1 promoter. The H1-p53-sh or the TetO7H1-p53-sh was introduced into the pLenti6-Block-IT plasmid through recombination (Invitrogen Clonase). *TP53* si, GACUCCAGUGGUAAUCUACTT; *SULF2* si#1, CCAUCAAUGAGACUCACAATT; *SULF2* si#2, GAGUGGGUCGGACUC-CUUATT.

Note: Supplementary data for this article are available at Cancer Research Online (http://cancerres.aacrjournals.org/).

Current address for P. Warrener: Targeted Growth, Inc., 1441 N 34th Street, Seattle, WA 98103. Current addresses for B.N. Chau, A.N. Chang and P.S. Linsley: Regulus Therapeutics, Carlsbad, CA 92008. B.N. Chau and R.L. Diaz contributed equally to this work.

Requests for reprints: Michele A. Cleary, Rosetta Inpharmatics LLC, 401 Terry Avenue North, Seattle, WA 98109. Phone: 206-802-6392; Fax: 206-802-6388; E-mail: michele_cleary@merck.com.

doi:10.1158/0008-5472.CAN-08-2742

Chemicals. Bleomycin, doxorubicin, and doxycycline were obtained from Sigma. Nutlin was obtained from Cayman Chemical. The active and inactive enantiomers were separated by supercritical-fluid chromatography using a Chiralcel OD-H column (Chiral Technology). Mouse monoclonal anti-FDXR antibody was purchased from Santa Cruz Biotechnology.

Tissue culture and cell line generation. Cell lines were obtained from American Type Culture Collection and cultured as recommended. To generate matched-pair lines and inducible cell lines, lentiviruses expressing p53-1026sh and tT-R were generated according to the manufacturer's (Invitrogen) protocol. Knockdown of *TP53* message level was determined by quantitative PCR.

RNA isolation and gene expression analysis. Total RNA was isolated by RNEasy (Qiagen) according to the manufacturer's instructions. Microarray analyses were done as previously described (17). Briefly, to identify the p53-regulated genes, ratios of transcript abundance in experimental versus control samples were calculated with normalized intensity data. Gene expression data analysis was done either with the Rosetta Resolver gene expression analysis software (Rosetta Biosoftware) or Matlab (The Mathworks). For each gene sequence on the arrays, statistical significance of differential gene expression was calculated according to the following equation: P value = $2 \times [1 - \mathrm{Erf}(|\mathrm{xdev}|)]$, where Erf is the error function for a Gaussian distribution of zero mean and xdev is the adjusted difference in fluorescence intensities between Cy3 and Cy5 intensities.

ChIP. Cell pellets were Dounce homogenized after formaldehyde fixing and glycine quenching. DNA was sheared to an average length of 300 to 500 bp by sonication and was precleared with protein A-agarose beads (Invitrogen). p53-bound DNA was isolated with antibodies against p53 (Santa Cruz sc-6243) and protein A-agarose beads. Complexes were washed and DNA was eluted from the beads followed by RNase and proteinase K treatment. ChIP DNA was purified by phenol-chloroform extraction and ethanol precipitation. For ChIP, quantitative PCR reactions were carried out in triplicate on specific genomic regions by use of SYBR Green Supermix (Bio-Rad). The resulting signals were normalized for primer efficiency by quantitative PCR for each primer pair with input DNA. Experimental C_t values were converted to copy numbers detected by comparison with a DNA standard curve run on the same PCR plates. Copy number values were then normalized for primer efficiency by dividing by the values obtained with input DNA and the same primer pairs. For ChIP-on-chip, ChIP, and input DNA, DNA was amplified by use of random priming amplification. Amplified DNA was fragmented and labeled by use of the DNA Terminal Labeling Kit from Affymetrix and then hybridized to Affymetrix GeneChip Human Tiling 2.0R array sets. Arrays were washed and scanned, and the resulting CEL files were analyzed by use of Affymetrix TAS software. Thresholds were selected, and the resulting BED files were analyzed by use of GenPathway software. Primer pair sequences and product location: Untr12, TGGACCTTTACCTGCTTTATCA; AGCAAGGACTAGGATGACAGAA; chr12:59,954,075–59,954,305. *FDXR*, CCCCACAGACCTCCGTATC; GCTGGAGAAGGGTGAGACTG; chr17:70,380,302–70,380,499. *SULF2*, TCCCAAATCAGGTCCAAATC; GAGGAGGACAGCATAGCAGTG; chr20:45,845,579–45,845,693.

Luciferase and β-galactosidase assays. *SULF2* promoter sequence containing the putative p53 consensus site was PCR amplified from human genomic DNA (PCR primer sequence: forward GTACTGAGCTCGAGCCAATCGTTAAGTATAGGAACG; reverse GTACTAGATCTGAAGTACACACAAAGCCCAAACCCC). PCR fragments were subcloned 5′ to the open reading frame of firefly luciferase (pGL4.23, Promega). Luciferase activity was measured according to the manufacturer's instructions. β-Galactosidase assays were done with Senescence Detection kit following the manufacturer's instructions (Calbiochem).

Results

To identify downstream transcriptional targets of p53, we analyzed the gene expression profiles of a panel of cancer cell lines (lung: A549 and NCI-H460, ovarian: OAW42 and A2780, liver: HepG2, and osteosarcoma: U2OS; all of which express wild-type p53) with sustained *TP53* silencing mediated by transduction of the cells with a lentiviral vector expressing an shRNA targeting *TP53* (16). Silencing of the *TP53* transcript in these cell lines was efficient (~20% *TP53* mRNA remaining compared with control; Fig. 1*A*; Supplementary Table S1). To confirm loss of p53 protein function in these cells, we conducted cell cycle analysis following exposure of the cells to DNA-damaging agents. As expected, in p53-deficient cells, p53-dependent G_1 arrest was not induced by doxorubicin, verifying loss of p53 function (data not shown). Whole genome gene expression profiling uncovered a set of transcripts that are down-regulated >1.3-fold with $P < 0.05$ in the p53-deficient lines compared with the corresponding wild-type lines (Fig. 1*A*; Supplementary Table S1). Annotation of this set of transcripts showed enrichment for genes involved in the DNA damage response, cell cycle, and apoptosis. To distinguish the genes in this set that are direct transcriptional targets of p53 from secondary effects, we performed microarray-based whole genome ChIP (ChIP-on-chip) as well as focused ChIP on promoter regions of selected candidate genes in one of the cell lines (18). We also interrogated ChIP binding sites for the presence of consensus p53 recognition sequences using the p53MH algorithm (7). Combining our results from ChIP, gene expression profiling, and p53MH analysis, we identified 32 genes whose expression is down-regulated in p53-deficient lines and that have p53-binding sites proximal to their promoter regions (Table 1). Of these 32 genes, two thirds overlap with or are highly connected to core p53 pathway genes (KEGG, Kyoto Encyclopedia of Genes and Genomes). The remaining one third represents putative novel direct transcriptional targets of p53.

From among this set of genes, we focused on studying the relationship between p53 and *SULF2* for the following reasons: (*a*) The results from the ChIP-on-chip experiment using untreated TOV21G cells and bioinformatics analyses show that there is a consensus p53 binding site in the first intron of *SULF2* (Fig. 1*B*). (*b*) Two recent reports studying the response of HCT116 p53 somatic knockout matched-pair lines to 5-fluorouracil as well as results with multiple cell lines treated with the p53 activator Nutlin are consistent with *SULF2* acting as a potential downstream target of p53 (4, 19). (*c*) Furthermore, overexpression of either SULF2 or SULF1 inhibited growth of myeloma xenografts in a previous study, providing support for the hypothesis that SULF2 has tumor suppressor function (15). To show that the *SULF2* promoter sequence contains a p53-binding site and can respond to activation of p53, we performed ChIP on cells exposed to DNA damage. As shown in Fig. 1*C*, an increase in the number of p53 binding events in the promoter regions of *SULF2* and *FDXR* (a known direct p53 transcriptional target) was observed compared with a random nontranscribed genomic locus. Such binding events were further increased in response to DNA damage. As expected, an increase of FDXR protein and stabilization of p53 was observed in response to genotoxic stress (Supplementary Fig. S1*A* and *B*). (Commercially available SULF2 antibodies did not detect a specific SULF2 band in immunoblot analysis).

For direct manipulation of the p53 response element in the *SULF2* promoter, we subcloned the 330-bp genomic region surrounding the putative p53 binding site into a luciferase reporter system. Nutlin is a small molecule that disrupts the interaction between p53 and its negative regulator MDM2 leading to p53 stabilization and activation (20). As shown in Fig. 1*D*, we observed a 3-fold increase in luciferase activity in response to treatment of cells with active Nutlin but not with an inactive enantiomer. As an additional control, in the p53 knockdown background, the *SULF2*

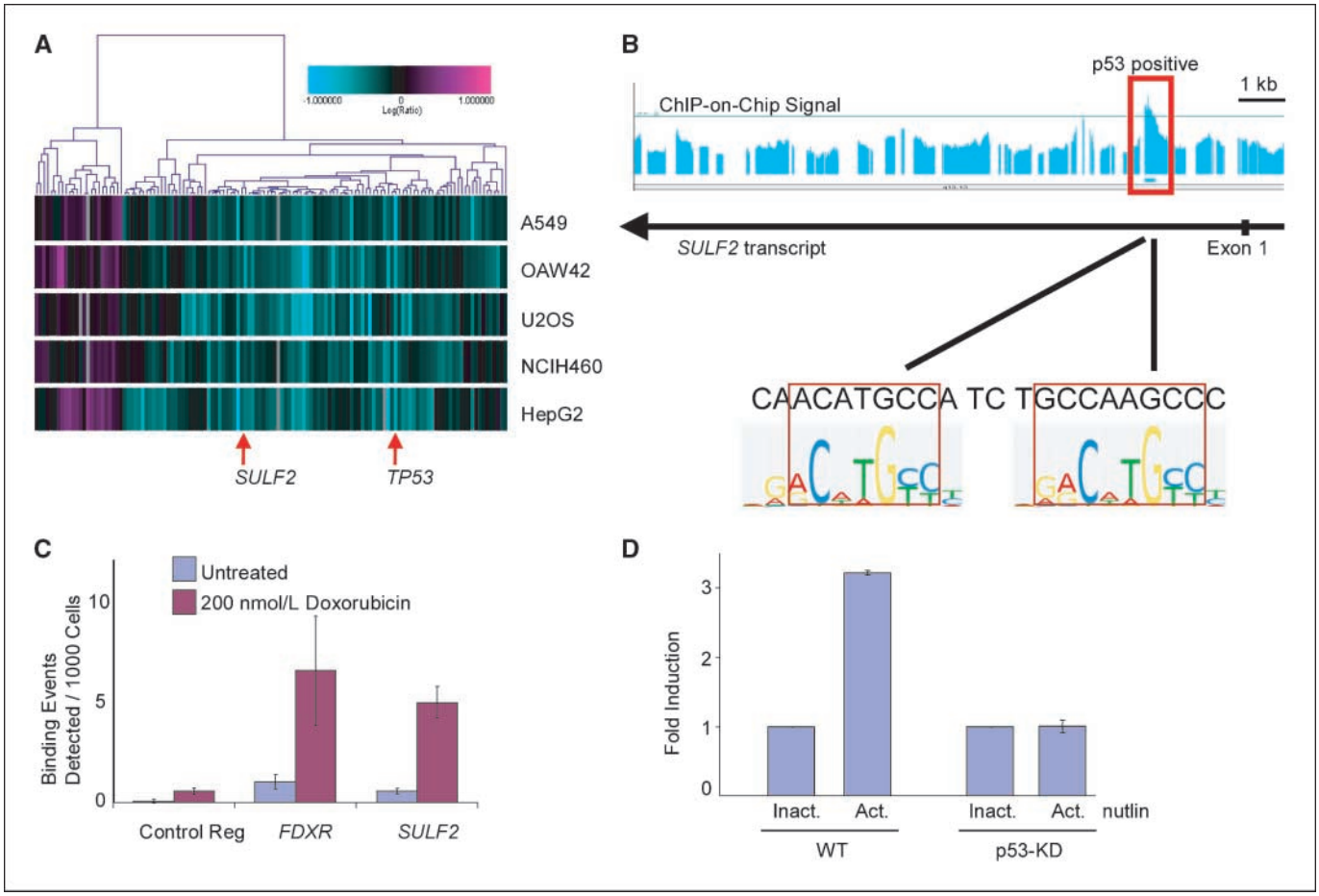

Figure 1. Identification of *SULF2* as a novel direct transcriptional target of p53. *A,* transcriptional profiles of p53-deficient cell lines of the indicated parental origin were compared with corresponding control lines. Shown are genes down-regulated ≥1.3-fold with $P < 0.05$. *Arrows, TP53* and *SULF2. B,* schematic of the *SULF2* genomic region (30 kb). *SULF2* intron 1 shows a positive signal above threshold in ChIP-on-chip analysis. *Red boxes,* sequence of the putative p53 binding site compared with the optimal p53 recognition sequence (25). *C,* focused ChIP interrogating promoter regions of *FDXR* (positive control) and *SULF2* in TOV21G cells. Compared with a nontranscribed region (control reg), the *SULF2* and *FDXR* promoters show an increase in the number of binding events in both untreated or doxorubicin-treated cells. *D,* activity of a luciferase reporter containing 330 bp of the *SULF2* promoter in A549 control [wild-type (*WT*)] and p53-deficient (*p53-KD*) lines. Cells were treated with 10 μmol/L active Nutlin or the inactive enantiomer.

genomic sequence did not confer transcriptional activity in the presence of Nutlin. Together, the results of gene expression profiling, ChIP, bioinformatic analyses, and luciferase assays led us to conclude that p53 binds to and activates transcription of the *SULF2* promoter.

Because direct transcriptional targets of p53 are up-regulated in response to DNA damage, we profiled gene expression changes in TOV21G ovarian carcinoma and A549 non–small cell lung carcinoma cells treated with doxorubicin. We collected RNA at various time points posttreatment to compare the kinetics and magnitude of *SULF2* induction (with 0 hour as baseline) with that of three well-established p53-regulated genes, *GADD45A, CDKN1A* (*p21*), and *FDXR*. As negative controls, transcript levels of three non–p53-regulated genes (*TP53, ATM*, and *CHEK2*) known to respond posttranscriptionally to DNA damage were determined. In both cell lines, *SULF2* induction occurred as early as 12 hours posttreatment and was sustained throughout the 24-hour treatment period. The fold induction of *SULF2* transcript was also generally comparable with changes in the three p53-regulated genes whereas transcript levels of the negative controls (*TP53, ATM*, and *CHEK2*) did not change in either cell line (Fig. 2*A*).

DNA damage–induced cellular stress induces changes in many transcripts irrespective of p53 status. To show that DNA damage–induced *SULF2* up-regulation is p53 dependent, we studied *SULF2* up-regulation in two different p53 matched-pair lines. We engineered HepG2 cells with tetracycline-regulatable knockdown of *TP53* that achieves >80% suppression of *TP53* mRNA on induction with doxycycline (data not shown). We compared expression changes in *SULF2* with that of the same three well-characterized p53 target genes in the p53 wild-type and p53-deficient lines. As shown in Fig. 2*B*, up-regulation of *SULF2* was dampened in p53-deficient lines in the presence of doxorubicin. Therefore, up-regulation of *SULF2* in response to DNA damage does depend on direct transcriptional regulation by p53.

In addition to DNA damage, p53 can be activated by inhibition of MDM2, which mediates the ubiquitination and subsequent proteolysis of p53. We used both genetic (RNAi) and pharmacologic approaches (Nutlin) to inhibit MDM2 function. First, we silenced *MDM2* by transfecting TOV21G and A549 cells with esiRNAs. esiRNAs comprise pools of small double-stranded RNA fragments generated from bidirectional transcription of a gene-specific cDNA followed by enzymatic digestion with RNase III optimized to yield siRNA-like fragments. This approach elicits potent RNAi of intended

Table 1. Direct transcriptional targets of p53

Members of or connected to KEGG p53 core pathway

Accession no.	Gene symbol
Contig43039_RC	*ALOX5*
NM_138763	*BAX*
NM_014417	*BBC3*
NM_020375	*C12orf5*
NM_000389	*CDKN1A*
NM_000107	*DDB2*
NM_152873	*FAS*
NM_004110	*FDXR*
NM_001924	*GADD45A*
NM_004864	*GDF15*
NM_000177	*GSN*
NM_001553	*IGFBP7*
NM_022767	*ISG20L1*
NM_012396	*PHLDA3*
NM_003463	*PTP4A1*
NM_015713	*RRM2B*
NM_007111	*TFDP1*
NM_147187	*TNFRSF10B*
NM_033285	*TP53INP1*
NM_006074	*TRIM22*
NM_152240	*ZMAT3*

Disconnected from KEGG p53 core pathway

Accession no.	Gene symbol
NM_004306	*ANXA13*
NM_152640	*DCP1B*
NM_001082	*CYP4F2*
NM_019000	*FAM134B*
NM_018194	*HHAT*
NM_014278	*HSPA4L*
NM_024430	*PSTPIP2*
NM_130843	*PTPRN2*
NM_015920	*RPS27L*
NM_145263	*SPATA18*
NM_018837	*SULF2*

targets and dilutes off-target effects for any given member of the pool (21). As shown in Fig. 3*A*, silencing of *MDM2* by esiRNAs generated from two distinct segments of the *MDM2* cDNA resulted in the up-regulation of known p53 targets as well as *SULF2*. Second, to pharmacologically perturb p53 function, we induced its activity by Nutlin. As shown in Fig. 3*B* and *C*, treatment with Nutlin, but not its inactive analogue, resulted in increases in *SULF2* and *p21* (positive control) expression levels that were dose dependent (Fig. 3*B*) and had similar kinetics (Fig. 3*C*). These observations lend further support for the direct regulation of *SULF2* by p53.

After establishing a molecular connection between p53 and *SULF2*, we investigated whether SULF2 protein participates in downstream functions of p53. It is well known that cellular senescence in response to genotoxic stress is p53 dependent. As shown in Fig. 4, cells exposed to doxorubicin or bleomycin underwent senescence as measured by increased β-galactosidase activity. However, when expression of *SULF2* or *TP53* (control) was silenced by RNAi, the number of cells showing signs of genotoxic stress-

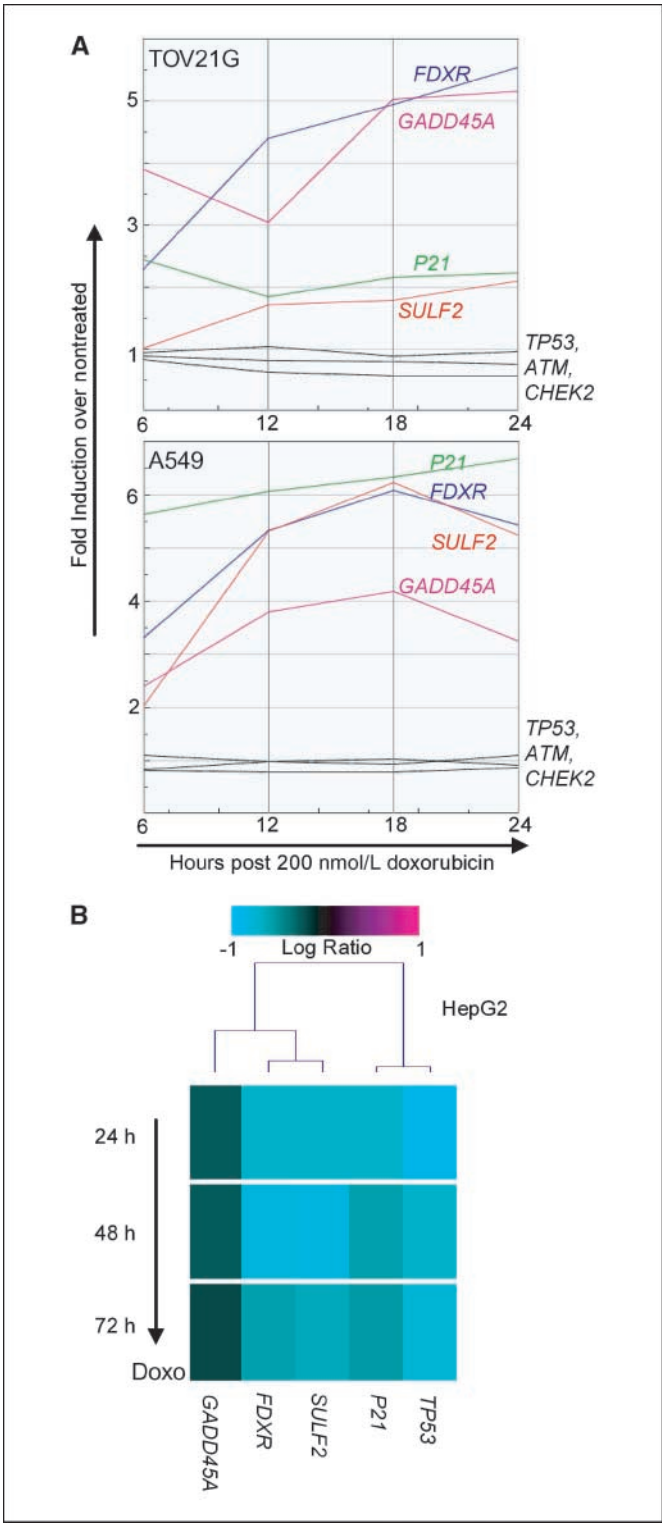

Figure 2. SULF2 up-regulation induced by DNA damage is p53 dependent. *A,* TOV21G and A549 cells were treated with 200 nmol/L doxorubicin, and RNA was collected at the indicated time points. Fold induction of transcripts was determined by comparison of RNA isolated from treated samples with that of corresponding untreated cells (0 h). *TP53, ATM*, and *CHEK2* negative control transcripts did not change. *B,* engineered HepG2 cells were left untreated or treated with 100 ng/mL doxycycline for 48 h to induce *TP53* silencing. Uninduced or induced cells were exposed to 200 nmol/L doxorubicin, and RNA was collected from samples at the indicated time points. As shown in the heat map, in the p53-deficient background, *TP53* was down-regulated and induction of p53 target genes in response to DNA damage (doxorubicin) was hampered.

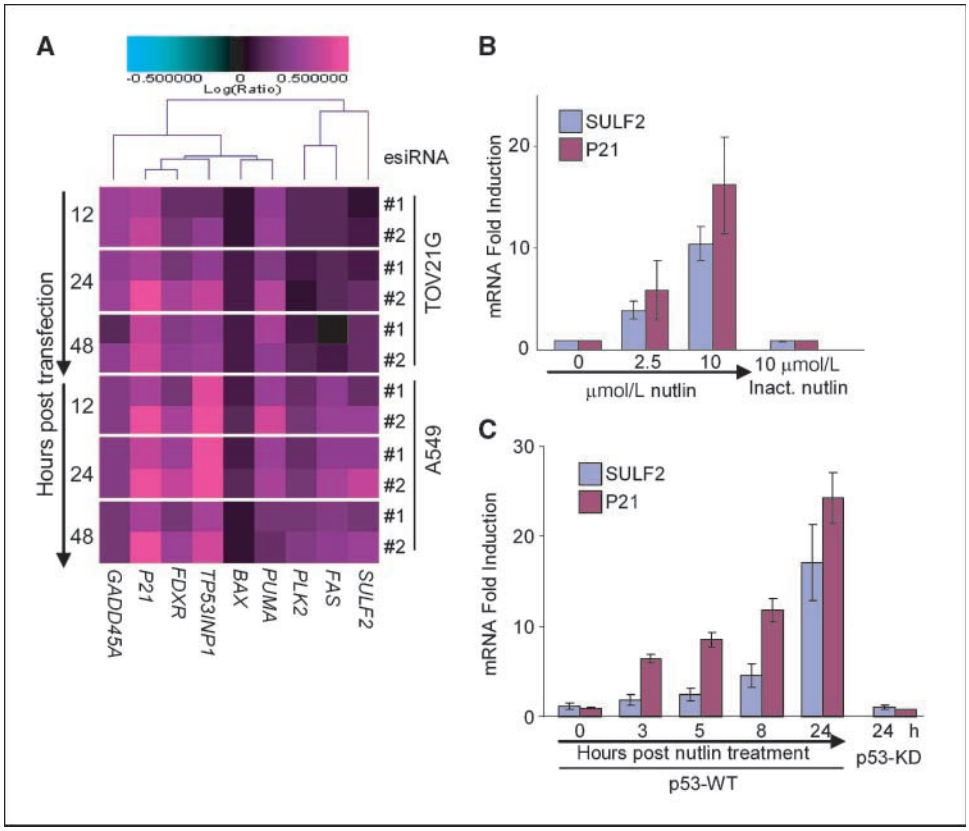

Figure 3. *SULF2* up-regulation induced by *MDM2* inhibition is p53 dependent. *A,* TOV21G and A549 cells were transfected with two different *MDM2* esiRNA pools targeting different regions of the *MDM2* transcript, and RNA was collected at the indicated time points. Gene expression of esiRNA-transfected cells was compared with that of mock-transfected cells. *B* and *C,* A549 p53-deficient and wild-type cells were treated with increasing doses of Nutlin for 24 h (*B*) or with 10 μmol/L Nutlin for the indicated times (*C*). *SULF2* and *p21* fold induction was determined by quantitative PCR [transcript levels at 0 μmol/L (*B*) or 0 h (*C*) were set to 1]. Response to inactive Nutlin (*B*) and transcript regulation in a p53-deficient cell line (*C*) served as negative controls.

induced senescence decreased. These data support the idea that *SULF2* is not only a direct target of p53 but also functions within the arm of the p53 tumor suppression pathway that leads to senescence.

Discussion

Gene expression profiling of matched-pair cell lines generated through RNAi-mediated knockdown of *TP53* provided us with a means to probe a defined genetic perturbation in an otherwise identical genetic background. Gene expression profiling identifies direct and indirect downstream effects of transcription factor perturbation, whereas ChIP can reveal the direct genomic binding sites of a factor. Similar to the concept of performing secondary and orthogonal assays to validate hits from a primary small molecule screen, coupling these technologies allowed us to uncover known, as well as novel, direct transcriptional targets of p53 with high confidence. Not only do the promoter regions of these genes contain p53 binding sites but also their expression is lost in response to p53 loss. Two thirds (21 of 32) of the genes have been shown to be directly involved in the currently understood core p53

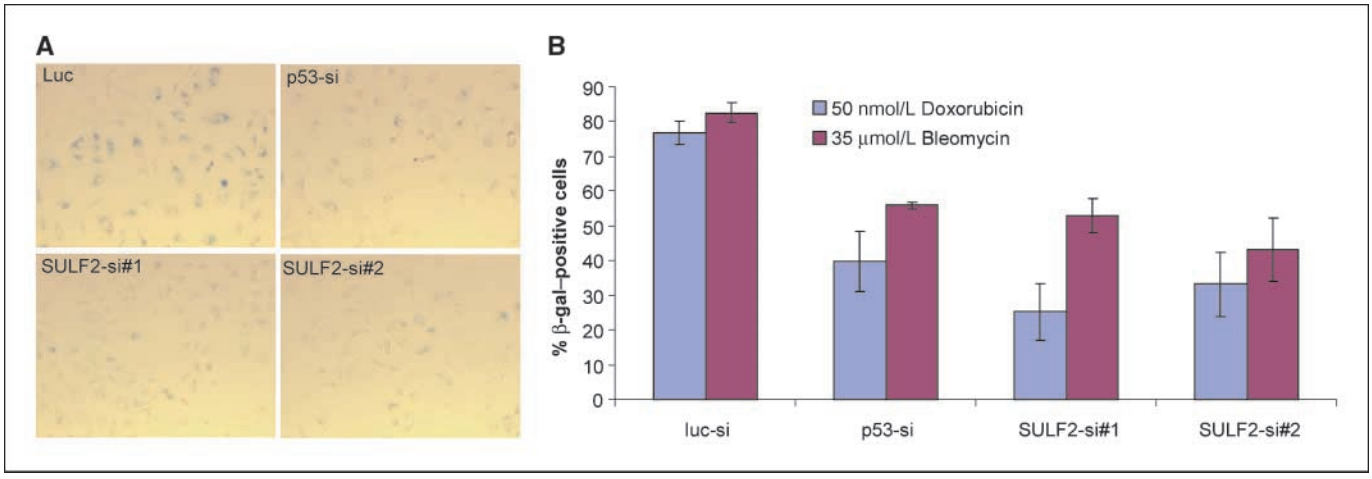

Figure 4. Senescene induced by p53 activation depends on SULF2. Activation of p53 leads to increase in growth factor signaling. A549 cells were transfected with siRNAs targeting *TP53* or *SULF2*. Twenty-four hours after transfection, cells were exposed to 50 nmol/L doxorubicin or 35 μmol/L bleomycin for 3 additional days. Cells were then fixed and stained for β-galactosidase (*β-gal*) activity. *A,* representative pictures of the doxorubicin-treated samples. *B,* percentage of β-galactosidase–positive cells (representative of four independent experiments) determined by counting >600 cells.

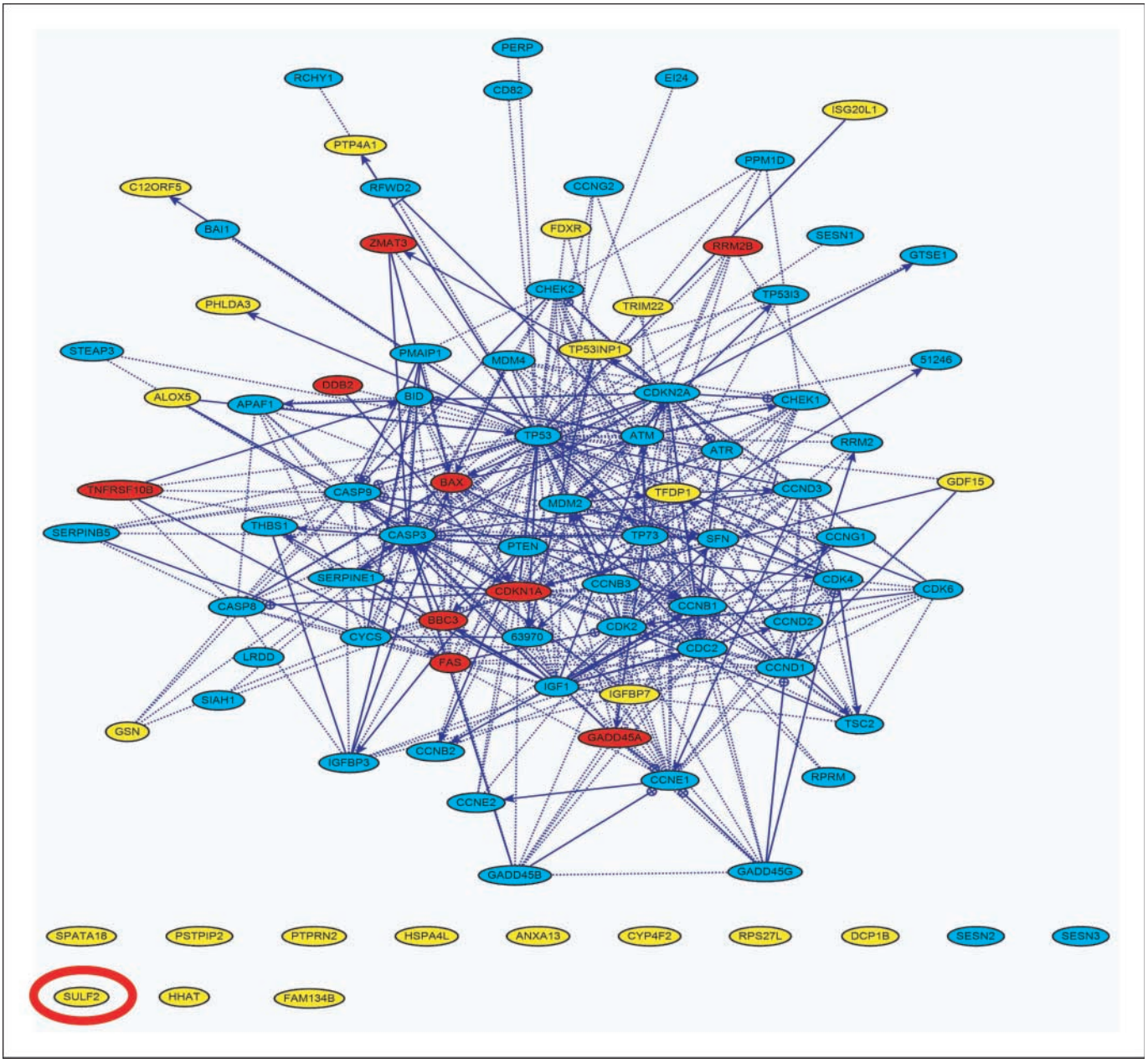

Figure 5. Network derived from interactions between the p53 pathway gene list defined by KEGG (26) and signature genes that overlapped in ChIP-on-chip assays. Edges were derived from protein-protein and regulatory interactions warehoused in BIND, BioGRID, DIP, HPRD, MINT, NetPro, Proteome, Reactome, the Rual et al. collection (27), Ingenuity, and GeneGo MetaBase. If the same edge was represented in multiple data sources, we collapsed the edges into a single edge to improve visualization (*dotted edges*). The node colors define which genes are from the p53 pathway (*blue nodes*), the signature (*yellow nodes*), and those that overlap between them (*red nodes*). Signature or pathway genes that did not connect were placed as orphan nodes at the bottom; *SULF2* was discovered in this collection of nodes.

pathway, and the remaining one third represent potentially novel downstream targets of p53 (Fig. 5; Table 1). Among these 11 target genes, we further validated p53-mediated regulation of *SULF2* and suggest a possible link between the p53 growth-suppressing function and the inhibitory role of SULF2 in growth factor signaling pathway.

Because SULF1 and SULF2 modulate growth factor signaling and are deregulated in various cancers, it is thought that aberrant sulfatase function may lead to neoplastic transformation. However, the precise role of these factors in tumorigenesis remains unclear. Overexpression of sulfatases in pancreatic cancers suggested that they regulate tumorigenesis by modulating WNT pathway signaling (11). A number of reports, however, showed that SULF1 loss is associated with a significant fraction of ovarian (75%), breast (60%), and liver cancers (30%; refs. 9, 13, 14). Moreover, reintroduction of SULF1 to hepatocellular cancer cells led to growth inhibition and increased sensitivity to apoptosis (9). Overexpression of SULF1 or SULF2 in a myeloma xenograft model also resulted in reduction of tumor growth (15). These seemingly contradictory findings could result from distinct cellular contexts such as cancer types and the relevant growth factor(s) of a particular tumor.

Our findings show that activation of p53 leads to the up-regulation of *SULF2*, and silencing of *SULF2* compromises cellular senescence induced by p53 activation. Taken together, these results support the notion that SULF2 acts as a downstream effector of p53 tumor suppressor function. Although mice with targeted disruptions in *Sulf1* or *Sulf2* revealed few developmental phenotypes, *Sulf1/Sulf2* knockout mice displayed neonatal/postnatal lethality associated with defects detected in multiple tissues (22–24). Breeding these mice into various tumor model contexts may lead to a better understanding of the role that these genes play in cancer.

Disclosure of Potential Conflicts of Interest

All authors are current or former employees of Merck & Co., Inc.

Acknowledgments

Received 7/22/2008; revised 10/23/2008; accepted 11/12/2008; published OnlineFirst 02/03/2009.

The costs of publication of this article were defrayed in part by the payment of page charges. This article must therefore be hereby marked *advertisement* in accordance with 18 U.S.C. Section 1734 solely to indicate this fact.

We thank Phieng Siliphaivanh (Merck Research Laboratory, Boston) for separating active Nutlin from its inactive analogue, GenPathway for performance of ChIP and ChIP-on-chip studies, the Rosetta Gene Expression Laboratory for microarray hybridizations, and members of the Rosetta Biology Department for assistance with this study.

References

1. Bartz SR, Zhang Z, Burchard J, et al. Small interfering RNA screens reveal enhanced cisplatin cytotoxicity in tumor cells having both BRCA network and TP53 disruptions. Mol Cell Biol 2006;26:9377–86.
2. Temam S, Flahault A, Perie S, et al. p53 gene status as a predictor of tumor response to induction chemotherapy of patients with locoregionally advanced squamous cell carcinomas of the head and neck. J Clin Oncol 2000; 18:385–94.
3. Liu MC, Gelmann EP, P53 gene mutations: case study of a clinical marker for solid tumors. Semin Oncol 2002; 29:246–57.
4. Kumamoto K, Spillare EA, Fujita K, et al. Nutlin-3a activates p53 to both down-regulate inhibitor of growth 2 and up-regulate mir-34a, mir-34b, and mir-34c expression, and induce senescence. Cancer Res 2008;68:3193–203.
5. Zhao R, Gish K, Murphy M, et al. Analysis of p53-regulated gene expression patterns using oligonucleotide arrays. Genes Dev 2000;14:981–93.
6. Mirza A, Wu Q, Wang L, et al. Global transcriptional program of p53 target genes during the process of apoptosis and cell cycle progression. Oncogene 2003;22: 3645–54.
7. Hoh J, Jin S, Parrado T, Edington J, Levine AJ, Ott J. The p53MH algorithm and its application in detecting p53-responsive genes. Proc Natl Acad Sci U S A 2002;99: 8467–72.
8. Lamanna WC, Kalus I, Padva M, Baldwin RJ, Merry CL, Dierks T. The heparanome-the enigma of encoding and decoding heparan sulfate sulfation. J Biotechnol 2007; 129:290–307.
9. Lai JP, Chien JR, Moser DR, et al. hSulf1 Sulfatase promotes apoptosis of hepatocellular cancer cells by decreasing heparin-binding growth factor signaling. Gastroenterology 2004;126:231–48.
10. Lai JP, Sandhu DS, Yu C, et al. R. Sulfatase 2 up-regulates glypican 3, promotes fibroblast growth factor signaling, and decreases survival in hepatocellular carcinoma. Hepatology 2008;47:1211–22.
11. Nawroth R, van Zante A, Cervantes S, McManus M, Hebrok M, Rosen SD. Extracellular sulfatases, elements of the Wnt signaling pathway, positively regulate growth and tumorigenicity of human pancreatic cancer cells. PLoS ONE 2007;2:e392.
12. Uchimura K, Morimoto-Tomita M, Bistrup A, et al. HSulf-2, an extracellular endoglucosamine-6-sulfatase, selectively mobilizes heparin-bound growth factors and chemokines: effects on VEGF, FGF-1, and SDF-1. BMC Biochem 2006;7:2.
13. Narita K, Chien J, Mullany SA, et al. Loss of HSulf-1 expression enhances autocrine signaling mediated by amphiregulin in breast cancer. J Biol Chem 2007;282: 14413–20.
14. Lai J, Chien J, Staub J, et al. Loss of HSulf-1 up-regulates heparin-binding growth factor signaling in cancer. J Biol Chem 2003;278:23107–17.
15. Dai Y, Yang Y, MacLeod V, et al. HSulf-1 and HSulf-2 are potent inhibitors of myeloma tumor growth *in vivo*. J Biol Chem 2005;280:40066–73.
16. Wiznerowicz M, Trono D. Conditional suppression of cellular genes: lentivirus vector-mediated drug-inducible RNA interference. J Virol 2003;77:8957–61.
17. Jackson AL, Bartz SR, Schelter J, et al. Expression profiling reveals off-target gene regulation by RNAi. Nat Biotechnol 2003;21:635–7.
18. Wei CL, Wu Q, Vega VB, et al. A global map of p53 transcription-factor binding sites in the human genome. Cell 2006;124:207–19.
19. Adamsen BL, Kravik KL, Clausen OP, De Angelis PM. Apoptosis, cell cycle progression and gene expression in TP53-depleted HCT116 colon cancer cells in response to short-term 5-fluorouracil treatment. Int J Oncol 2007;31: 1491–500.
20. Vassilev LT, Vu BT, Graves B, et al. *In vivo* activation of the p53 pathway by small-molecule antagonists of MDM2. Science 2004;303:844–8.
21. Kittler R, Surendranath V, Heninger AK, et al. Genome-wide resources of endoribonuclease-prepared short interfering RNAs for specific loss-of-function studies. Nat Methods 2007;4:337–44.
22. Holst CR, Bou-Reslan H, Gore BB, et al. Secreted sulfatases Sulf1 and Sulf2 have overlapping yet essential roles in mouse neonatal survival. PLoS ONE 2007;2:e575.
23. Ai X, Kitazawa T, Do AT, Kusche-Gullberg M, Labosky PA, Emerson CP, Jr. SULF1 and SULF2 regulate heparan sulfate-mediated GDNF signaling for esophageal innervation. Development 2007;134:3327–38.
24. Ratzka A, Kalus I, Moser M, Dierks T, Mundlos S, Vortkamp A. Redundant function of the heparan sulfate 6-*O*-endosulfatases Sulf1 and Sulf2 during skeletal development. Dev Dyn 2008;237:339–53.
25. el-Deiry WS, Kern SE, Pietenpol JA, Kinzler KW, Vogelstein B. Definition of a consensus binding site for p53. Nat Genet 1992;1:45–9.
26. Ogata H, Goto S, Sato K, Fujibuchi W, Bono H, Kanehisa M. KEGG: Kyoto encyclopedia of genes and genomes. Nucleic Acids Res 1999;27:29–34.
27. Rual JF, Venkatesan K, Hao T, et al. Towards a proteome-scale map of the human protein-protein interaction network. Nature 2005;437:1173–8.